

Inhibitive formation of nanocavities by introduction of Si atoms in Ge nanocrystals produced by ion implantation

R. S. Cai, Y. Q. Wang, L. Shang, X. H. Liu, Y. J. Zhang, G. G. Ross, and D. Barba

Citation: [Journal of Applied Physics](#) **115**, 204310 (2014); doi: 10.1063/1.4880661

View online: <http://dx.doi.org/10.1063/1.4880661>

View Table of Contents: <http://scitation.aip.org/content/aip/journal/jap/115/20?ver=pdfcov>

Published by the [AIP Publishing](#)

Articles you may be interested in

[The use of nanocavities for the fabrication of ultrathin buried oxide layers](#)

Appl. Phys. Lett. **94**, 011903 (2009); 10.1063/1.3065478

[Role of C in the formation and kinetics of nanovoids induced by He + implantation in Si](#)

J. Appl. Phys. **104**, 023501 (2008); 10.1063/1.2955707

[Dissociation of Si + ion implanted and as-grown thin SiO₂ layers during annealing in ultra-pure neutral ambient by emanation of SiO](#)

J. Appl. Phys. **101**, 053516 (2007); 10.1063/1.2436834

[Nanocrystal formation in SiC by Ge ion implantation and subsequent thermal annealing](#)

J. Appl. Phys. **91**, 1520 (2002); 10.1063/1.1430539

[Two-dimensional network of dislocations and nanocavities in hydrogen-implanted and two-step annealed silicon](#)

Appl. Phys. Lett. **72**, 2544 (1998); 10.1063/1.121413



Re-register for Table of Content Alerts

Create a profile.



Sign up today!



Inhibitive formation of nanocavities by introduction of Si atoms in Ge nanocrystals produced by ion implantation

R. S. Cai,¹ Y. Q. Wang,^{1,2,a)} L. Shang,¹ X. H. Liu,¹ Y. J. Zhang,¹ G. G. Ross,³
 and D. Barba^{3,a)}

¹The Cultivation Base for State Key Laboratory, Qingdao University, No. 308 Ningxia Road, Qingdao 266071, People's Republic of China

²College of Physics Science, Qingdao University, No. 308 Ningxia Road, Qingdao 266071, People's Republic of China

³INRS-Énergie, Matériaux et Télécommunications, 1650 boulevard Lionel-Boulet, Varennes Québec J3X 1S2, Canada

(Received 8 March 2014; accepted 19 May 2014; published online 29 May 2014)

Germanium nanocrystals (Ge-nc) were successfully synthesized by co-implantation of Si and Ge ions into a SiO₂ film thermally grown on (100) Si substrate and fused silica (pure SiO₂), respectively, followed by subsequent annealing at 1150 °C for 1 h. Transmission electron microscopy (TEM) examinations show that nanocavities only exist in the fused silica sample but not in the SiO₂ film on a Si substrate. From the analysis of the high-resolution TEM images and electron energy-loss spectroscopy spectra, it is revealed that the absence of nanocavities in the SiO₂ film/Si substrate is attributed to the presence of Si atoms inside the formed Ge-nc. Because the energy of Si-Ge bonds (301 kJ·mol⁻¹) are greater than that of Ge-Ge bonds (264 kJ·mol⁻¹), the introduction of the Si-Ge bonds inside the Ge-nc can inhibit the diffusion of Ge from the Ge-nc during the annealing process. However, for the fused silica sample, no crystalline Si-Ge bonds are detected within the Ge-nc, where strong Ge outdiffusion effects produce a great number of nanocavities. Our results can shed light on the formation mechanism of nanocavities and provide a good way to avoid nanocavities during the process of ion implantation. © 2014 AIP Publishing LLC.

[<http://dx.doi.org/10.1063/1.4880661>]

I. INTRODUCTION

In recent years, nanostructured Ge embedded in SiO₂ has received considerable attention, because of its greater absorption efficiency over the complete visible spectrum for extended photovoltaic applications.^{1,2} However, the high thermal diffusivity of Ge atoms within silica glass induces a strong Ge desorption above 1000 °C, which can drastically limit the integration of Ge nanocrystals (Ge-nc) into third generation solar cells or other luminescent devices.³⁻⁵ Such a feature is generally accompanied by the formation of nanocavities, which seems to be preceded by the formation of Ge-nc.⁵ Although some researchers have evoked oxidization effects associated with the formation of highly mobile GeO molecules,⁶ the mechanisms responsible for the Ge outdiffusion and the subsequent formation of nanocavities remain unclear.

To increase the quantity of retained Ge in the SiO₂ matrix, the use of Si co-implantation has been proposed in our previous study, because the introduction of excessive Si into the oxide matrix can trap a great number of diffusing Ge atoms during high temperature treatment.^{7,8} Although the increase of the retained Ge is attributed to the formation of large aggregates containing a mixture of Ge-Ge, Si-Ge, and Si-Si atom chains, the chemical composition of the Ge-nc has not been clarified yet. At present, it is very challenging

to prepare cross-sectional specimens of the fused silica and SiO₂ film/Si substrate for transmission electron microscopy (TEM) observation, so the investigation concerning the co-implantation system is usually carried out using scanning electron microscopy (SEM). TEM examinations on the co-implantation system are highly desired for understanding the microstructure and chemical composition of the Ge-nc. Our recent Rutherford backscattering spectroscopy (RBS) measurements show that the Ge desorption is less than 50% for Ge-nc in the SiO₂ film grown on (100) Si, while more than 90% Ge desorption takes place in the fused silica annealed at 1150 °C.⁸ This unexplained phenomenon motivates us to carry out in-depth study of the Ge-nc produced in these systems, using various approaches to identify the differences of their microstructures and/or their chemical compositions.

In this paper, the microstructure of the Ge-nc produced by co-implantation of Si and Ge ions into the fused silica and SiO₂ film/Si substrate is investigated by high-resolution TEM (HRTEM). It shows that nanocavities only exist in the fused silica but not in the SiO₂ film/Si substrate. Electron energy-loss spectroscopy (EELS) is employed to clarify the chemical composition of the Ge-nc. It demonstrates that the Si atoms only exist in the Ge-nc within the SiO₂ film on a Si substrate, while most Ge-nc within the fused silica are composed of pure Ge atoms. The absence of nanocavity in SiO₂ film/Si substrate is attributed to the formation of Si-Ge bonds in the Ge-nc, which inhibits the outdiffusion of Ge atoms in Ge-nc.

^{a)}Authors to whom correspondence should be addressed. Electronic addresses: yqwang@qdu.edu.cn. Tel.: +86-532-83780318 and barba@emt.inrs.ca.

II. EXPERIMENTAL METHODS

The SiO₂ film with a thickness of ~150 nm was thermally grown on a (100) Si substrate at 1100 °C by dry oxidation method. The ion implantation and annealing conditions were the same for both fused silica and SiO₂ film/Si substrate samples. The ²⁸Si⁺ ions were first implanted with a fluence of $7 \times 10^{16} \text{ cm}^{-2}$ at an acceleration voltage of 50 kV. Then the ⁷⁴Ge⁺ implantation was performed with a fluence of $8 \times 10^{16} \text{ cm}^{-2}$, at an acceleration voltage of 70 kV, providing an implantation depth distribution similar to that at 50 kV for Si. The samples were subsequently annealed at 1150 °C for 1 h, under ultrahigh pure N₂ atmosphere.

Cross-sectional specimens for TEM observations were prepared using conventional techniques of mechanical polishing and ion-thinning. The ion thinning was carried out using Gatan model 691 precision ion polishing system. Selected-area electron diffraction (SAED), bright field (BF) and HRTEM were carried out using a JEOL JEM2100F TEM operating at 200 kV. EELS was performed on an FEI Tecnai F20 TEM. All the EELS spectra were acquired in the image mode with an electron beam probe size of 1–2 nm and half collection angle of ~16 mrad.

III. RESULTS AND DISCUSSION

Fig. 1(a) shows a typical cross-sectional BF TEM image of the fused silica sample. It can be clearly seen that two kinds of nano-objects can be identified, which are located in the region from the top surface to a depth of 90 nm. The dark and bright objects correspond to Ge-nc and nanocavities, respectively. Their shapes are almost spherical, and their diameters vary from 5 to 70 nm. This indicates that the formation of big Ge-nc is owing to Ostwald ripening effect. Both the spatial distributions and geometry of Ge-nc are similar to those observed by SEM in our previous work.⁵ In Fig.

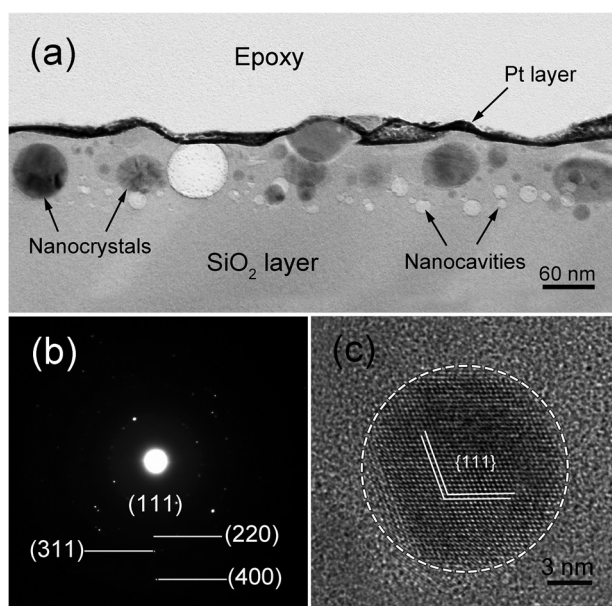


FIG. 1. (a) Cross-sectional BF TEM image of the fused silica sample; (b) SAED pattern taken from the Ge-ncs embedded in SiO₂ matrix; (c) Typical HRTEM image of a single Ge nanocrystal.

1(a), the dark Pt layer is deposited on the surface of fused silica to show the free surface more clearly. It can be seen that the free surface of the Pt layer is not flat, and some islands can be seen obviously. This may result from the swelling effect.⁹ The annealing temperature is 1150 °C which is much higher than the melting point of the Ge (937 °C), thus Ge-nc will experience a phase transition from liquid to solid, which leads to a volume expansion on the surface of the sample. Fig. 1(b) is a typical SAED pattern taken from the Ge-nc embedded in the SiO₂ matrix, which can be indexed using the lattice parameter ($a = 5.658 \text{ \AA}$) of Ge. Fig. 1(c) is a typical HRTEM image of a single Ge nanocrystal with a diameter of about 15 nm. The interplanar spacing of the lattice planes marked by two pairs of parallel white lines in Fig. 1(c) is measured to be 3.26 Å, which is consistent with the spacing of {111} planes of Ge ($d_{111} = 3.267 \text{ \AA}$).

Fig. 2(a) shows a typical BF TEM image of a cross-sectional SiO₂ film grown on a Si substrate. The free surface of the sample is marked by two horizontal black arrows. As expected, the thickness of the SiO₂ film is about 150 nm. By comparing Fig. 2(a) with Fig. 1(a), it can be seen that the amount of the Ge-nc (dark objects) is greater in the SiO₂ film/Si substrate than that in the fused silica, which reflects the higher desorption of Ge in the fused silica. The nanocrystals formed in the SiO₂ film are contained within a depth of 0–80 nm, which is consistent with the depth profile of implanted ions inside the target.¹⁰ Besides some big Ge-nc located near the free surface of sample, many small ones are also observed at a deeper depth. The shape of the big Ge-nc is not spherical but elongated and elliptical, while the small ones are nearly spherical. The formation of the big Ge-nc is due to Ostwald ripening effect and/or coalescence of small neighboring Ge-nc during the annealing process. After careful examination of the whole sample, it is interesting to note that no nanocavity is detected. Fig. 2(b) is the SAED pattern obtained from the nanocrystals embedded in the SiO₂ matrix. The diffraction rings can also be indexed using the lattice

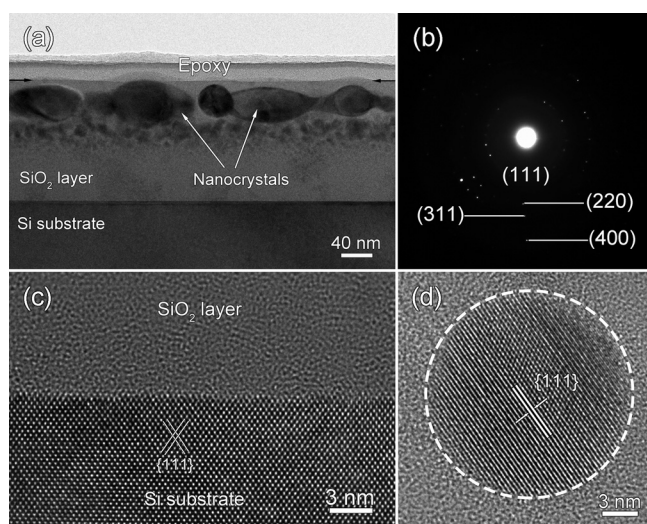


FIG. 2. (a) Cross-sectional BF TEM image of the SiO₂ film on a Si substrate; (b) SAED pattern taken from the Ge-nc embedded in SiO₂ matrix; (c) HRTEM images of the interface between Si substrate and SiO₂ matrix (c) and a perfect Ge nanocrystal (d), respectively.

parameter ($a = 5.658 \text{ \AA}$) of Ge. However, the interplanar spacings measured from the diffraction rings are slightly smaller than the theoretical values. Fig. 2(c) is the [110] zone-axis HRTEM image of the interface between the Si substrate and the SiO₂ layer. Fig. 2(d) shows a typical HRTEM image of a single Ge nanocrystal with a diameter of 17 nm. The interplanar spacing of the lattice plane marked by a pair of parallel lines is measured to be 3.19 Å, which is smaller than the theoretical value ($d_{111} = 3.267 \text{ \AA}$), consistent with the SAED results. This might be caused by the existence of Si in Ge-nc forming some Si-Ge bonds ($r = 2.40 \text{ \AA}$) shorter than Ge-Ge bonds ($r = 2.44 \text{ \AA}$).

Si and Ge have a significant miscibility due to their similarity in crystal structures and the slight difference in lattice parameters ($a_{\text{Si}} = 5.432 \text{ \AA}$, $a_{\text{Ge}} = 5.658 \text{ \AA}$). The interplanar spacings of Si (111) lattice planes and Ge (111) lattice planes are 3.136 Å and 3.267 Å, respectively. The small distinction makes it very hard to distinguish whether Si exists in Ge-nc only from HRTEM images. So EELS analysis is employed to investigate the difference of the chemical composition for the Ge-nc inside the two samples. This approach has been used to study the electronic structure of Si nanocrystals embedded in SiO₂ matrix by Wang *et al.*¹¹ Fig. 3(a) shows the background-subtracted EELS spectra obtained from a region without Si nanocrystals (upper panel) and from a region with Si nanocrystals (lower panel).¹¹ The EELS spectra obtained from the Ge-nc in fused silica and SiO₂ film/Si substrate are shown in Figs. 3(b) and 3(c), respectively. The data were recorded at the center of big Ge-nc at a depth of ~50 nm in both studied samples, to prevent any possible experimental artifacts related to Ge-nc interface effects and/or changes in the chemical composition of the surrounding oxide. For Ge-nc embedded in the SiO₂ film, between 95 and 100 eV, a clear peak (P) is found at ~100 eV, which is compatible with the $L_{2,3}$ edge of pure Si. In contrast, for Ge-nc in fused silica, no evident peak can be observed between 95 and 100 eV. By examining the Ge-nc in many other regions using EELS analysis, we conclude that most Ge-nc formed in the SiO₂ film/Si substrate contain Si atoms, whereas the Ge-nc produced in fused silica are almost exclusively composed of Ge

atoms. As for the origin of the Si atoms, we think the Si atoms inside the Ge-nc come from Si ions co-implantation. Some researchers¹²⁻¹⁴ reported that the free Si atoms can diffuse from the Si substrate to SiO₂ matrix or Ge-nc inside the SiO₂ matrix. However, in their experiments, the diffusion can only happen in the region near the surface of Si substrate. In our case, the thickness of the SiO₂ film is around 150 nm, and the distance from the surface of the Si substrate to the deepest Ge-nc layer is measured to be approximately 70 nm. Such a distance cannot enable free Si atoms to diffuse from Si substrate to Ge-nc.

Based on our experimental results and some relevant literature,⁴ we think that the formation of nanocavities is attributed to the outdiffusion of Ge atoms from Ge-nc in fused silica sample. After the ion co-implantation of Si⁺ and Ge⁺ ions into fused silica, some Si-O bonds are broken and some Si-Ge-O mixture bonds form including Ge-Ge, Ge-O, Si-Si, Si-Ge, and individual dangling bonds. At the initial stage of annealing treatment, local Ge concentration is high enough to form tiny Ge nanoclusters. The growth of Ge-nc is due to Ostwald ripening effect involving the dissolution of small clusters and the diffusion of small clusters towards large clusters atom by atom. As we all know, the diffusion ability of Ge in the SiO₂ matrix is very high at 1150 °C, so Ge atoms can diffuse from the Ge-nc to the free surface of the fused silica quickly and easily. The outdiffusion of Ge can result in the formation of vacancy clusters inside the Ge-nc. With the increase of annealing time, vacancy clusters become larger and larger, and nanocavities will eventually form in the SiO₂ matrix.

From the analysis of the above two samples, a distinct difference is that the nanocavities are only produced in the fused silica but not in the SiO₂ film/Si substrate. EELS analysis reveals that Si atoms exist in the most Ge-nc within the SiO₂ film, while the Ge-nc produced in the fused silica are almost composed of pure Ge atoms. Combining TEM observations with EELS analysis, it is believed that the presence of Si atoms inside Ge-nc can inhibit the formation of nanocavities. Our recent work¹⁵ has shown that the chemical environment for fused silica and SiO₂ film/Si substrate is remarkably different. Our x-ray photoelectron spectroscopy (XPS) analysis demonstrates that the fractions of silicon dangling bonds are 1% ± 1% and 13% ± 2%, respectively, in the pristine fused silica and SiO₂ film/Si substrate. After the ion implantation, the fractions of Si⁴⁺ are measured to be 70% ± 2% and 84% ± 2% in SiO₂ film/Si substrate and fused silica samples, respectively. This indicates that there is still approximately 13%–14% more Si bonded with four oxygen atoms in the fused silica than that in SiO₂ film/Si substrate. In other words, the percentage of dangling bonds in SiO₂ film/Si substrate is 13%–14% greater than that in the fused silica. During the annealing process, the silicon dangling bonds can bond with Ge atoms and form Si-Ge nanocrystals. Due to the greater percentage of silicon dangling bonds in SiO₂ film than that in fused silica, it is much easier to form Si-Ge nanocrystals in SiO₂ film. This deduction is consistent with our EELS results that most Ge-nc formed in the SiO₂ film contain Si atoms, whereas the Ge-nc produced in fused silica are almost exclusively composed of Ge atoms.

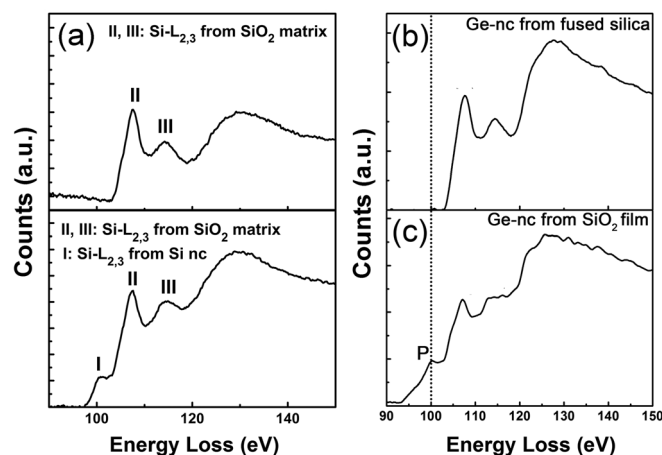


FIG. 3. (a) EELS spectra acquired from the regions without Si nanocrystal and with Si nanocrystal. Reprinted with permission from Wang *et al.*, Phys. Rev. B **71**, 161310(R) (2005). Copyright 2005 American Physical Society; EELS spectra obtained from the Ge-nc in fused silica (b) and SiO₂ film (c).

As for the trapping mechanism evoked to explain the effects of Si on the reduction of the Ge diffusivity,^{7,8} the incorporation of Si into Ge-Ge chains could significantly improve the thermal stability of Ge-nc. As we all know, the chemical bond energy of Si-Ge bond ($301 \text{ kJ}\cdot\text{mol}^{-1}$) is larger than that of the Ge-Ge bond ($264 \text{ kJ}\cdot\text{mol}^{-1}$). During the annealing process, the introduction of Si atoms in the Ge-nc can inhibit the outward diffusion of Ge from Ge-nc containing Si atoms. This would thus prevent the formation of nanocavities within the thermal SiO_2 film.

IV. CONCLUSION

In conclusion, the presence of Si atoms inside Ge-nc can significantly improve their stability at high temperatures. For fused silica samples, where no Si atoms are found in the Ge-nc, the release of Ge from the nanoparticles generates a great number of nanocavities. Whereas for the Ge-nc synthesized within a thermal SiO_2 film grown on a Si substrate, the presence of Si atoms inside the formed nanoparticles can prevent the release of Ge from Ge-nc, due to the hardening of internal Ge-Si chemical bonds.

ACKNOWLEDGMENTS

The authors would like to acknowledge the financial support from the National Key Basic Research Development Program of China (Grant No. 2012CB722705), the Natural Science Foundation for Outstanding Young Scientists in

Shandong Province (Grant No. JQ201002), the Program for Foreign Cultural and Educational Experts (Grant Nos. W20123702084 and W20133702021). Y. Q. Wang would also like to thank the financial support from Top-notch Innovative Talent Program of Qingdao City and the Taishan Outstanding Overseas Scholar Program of Shandong Province.

¹M. C. Beard, K. P. Knutsen, P. Yu, J. M. Luther, Q. Song, W. K. Metzger, R. J. Ellingson, and A. J. Nozik, *Nano Lett.* **7**, 2506 (2007).

²M. T. Trinh, R. Limpens, W. D. A. M. de Boer, J. M. Schins, L. D. A. Siebbeles, and T. Gregorkiewicz, *Nature Photon.* **6**, 316 (2012).

³M. V. Minke and K. A. Jackson, *J. Non-Cryst. Solids* **351**, 2310 (2005).

⁴E. S. Marstein, A. E. Gunnæs, U. Serincan, S. Jørgensen, A. Olsen, R. Turan, and T. G. Finstad, *Nucl. Instrum. Methods B* **207**, 424 (2003).

⁵D. Barba, F. Martin, J. Demarche, G. Terwagne, and G. G. Ross, *Nanotechnology* **23**, 145701 (2012).

⁶V. Beyer and J. von Borany, *Phys. Rev. B* **77**, 014107 (2008).

⁷D. Barba, J. Demarche, F. Martin, G. Terwagne, and G. G. Ross, *Appl. Phys. Lett.* **101**, 143107 (2012).

⁸D. Barba, J. Demarche, F. Martin, G. Terwagne, and G. G. Ross, *J. Appl. Phys.* **114**, 074306 (2013).

⁹W. K. Choi, V. Ho, V. Ng, Y. W. Ho, S. P. Ng, and W. K. Chim, *Appl. Phys. Lett.* **86**, 143114 (2005).

¹⁰J. Biersack and L. Haggmark, *Nucl. Instrum. Method* **174**, 257 (1980).

¹¹Y. Q. Wang, R. Smirani, G. G. Ross, and F. Schiettekatte, *Phys. Rev. B* **71**, 161310(R) (2005).

¹²Y. Maeda, *Phys. Rev. B* **51**, 1658 (1995).

¹³J. G. Zhu, C. W. White, J. D. Budai, S. P. Withrow, and Y. Chen, *J. Appl. Phys.* **78**, 4386 (1995).

¹⁴N. Jiang, J. Qiu, and J. C. H. Spence, *Appl. Phys. Lett.* **86**, 143112 (2005).

¹⁵D. Barba, R. S. Cai, J. Demarche, Y. Q. Wang, G. Terwagne, F. Rosei, F. Martin, and G. G. Ross, *Appl. Phys. Lett.* **104**, 111901 (2014).